All-optical delay line based on a cavity soliton laser with injection

C. McIntyre,* A. M. Yao, and G.-L. Oppo
SUPA and Department of Physics, University of Strathclyde, Glasgow G4 ONG, Scotland, United Kingdom

F. Prati and G. Tissoni
CNISM and INFM–CNR, Dipartimento di Fisica e Matematica, Università dell'Insubria, via Valleggio 11, I-22100 Como, Italy
(Received 27 October 2009; published 29 January 2010)

The motion and position of cavity solitons in a vertical-cavity surface-emitting laser with optical injection are investigated. Spatial variations of the phase of the injected field are considered in the form of sinusoidal and triangular modulations. We show how the velocity, distance traveled, and final position of the cavity solitons can be controlled by varying the slope of the phase modulations and the response time of the semiconductor medium. Numerical simulations demonstrate the feasibility of an all-optical delay line in a cavity soliton laser. Merging of cavity solitons is observed when they collide at modulation maxima and is shown to be beneficial in the operation of the delay line. The merging and consequent emission of pulsed and localized light is explained in terms of violation of energy balance for soliton systems in the presence of injection and dissipation.

DOI: 10.1103/PhysRevA.81.013838 PACS number(s): 42.65.Sf, 85.30.De, 05.10.−a, 42.55.Ah

I. INTRODUCTION

Cavity solitons (CS) and, more generally, spatial dissipative solitons [1,2] are independent and controllable localized light peaks on a low-intensity, homogeneous (or quasihomogeneous) background. They have been described in a variety of models in photonics and observed, more notably, in both single feedback mirror experiments [3] and semiconductor microresonators [4]. More recently, attention has moved from passive to active systems with the specific aim of realizing a "cavity soliton laser" (CSL). This objective has been achieved in different configurations, from vertical-cavity surface-emitting lasers (VCSELs) with optical injection [5,6] to VCSELs with frequency-selective feedback [7,8] and coupled VCSEL resonators [9].

In terms of practical applications, CS features such as their ability to be independently written and erased were first used in optical memories [2,10]. These features have been combined with the motion of CS in phase gradients to build an all-optical delay line with a high figure of merit [11]. In this, a pulsed input signal creates (writes) a sequence of CS that is quickly moved away from its original position via a background phase gradient. CS are then read out at the end of the line either by a sequence of pulses with an appropriate erasing phase or by well-localized detectors.

All-optical delay lines based on CS have thus far been demonstrated in *passive* configurations [2,11] and only limited attention has been devoted to the readout operation of the delay line. The aim of this article is to demonstrate the feasibility of an all-optical delay line in an *active* configuration: a CS laser with injection. Our first step is to obtain reduced models describing VCSELs with optical injection, following a recent method to eliminate stiffness in laser equations [12]. We then investigate the use of phase modulations of the injected field to move CS in the transverse space and to control their final position at the maxima of the modulation. The readout operation is achieved in the modulation extrema by the merging of CS and the release of light pulses that can be detected over a broad area, thus replacing the use of erasing pulses. CS merging features are favored in the CSL with injection with respect to other systems [2] because of the absence of spatial oscillations in the CS tails.

The article is organized as follows: In Sec. II we introduce the dynamical Maxwell-Bloch equations that describe the VCSEL with optical injection and discuss under which conditions and to what extent the equations can be simplified by taking advantage of the separation of the time scales of the different variables. The final models are highly efficient for numerical integration and allow for a systematic investigation of the delay line for the chosen parameter values. Section III details the optimization of the duration and separation of the input pulses superimposed onto the injected signal in order to generate sequences of CS in the delay line. Numerical simulations are performed in both one-dimensional (1D) and two-dimensional (2D) transverse-space configurations. Control of the CS motion, velocity, and position by the shape of the phase modulation of the injected field is investigated in Sec. IV. In particular, we study sinusoidal and triangular modulations of the input phase. Section V is devoted to the investigation of the phenomenon of CS merging that occurs when two CS move toward the same spatial position at the peak of the phase modulation. By extending energy balance considerations to CS in the presence of injection and dissipation, we demonstrate that such merging processes are accompanied by the emission of short pulses of light that can be collected and used as the output of the delay line. Merging strongly reduces the CS clogging close to the readout position that may detrimentally affect delay lines in passive systems. Merging is, in fact, favored in CSL because CS in lasers have almost no spatial oscillations in their tails. Conclusions and discussion of the relevance of our results to the realization of delay lines based on CSL are presented in Sec. VI. We predict that all-optical delay lines with CS lasers can operate at typical speeds of Gb/s with delays that are limited only by the transverse size of the VCSEL sample.

*craig.mcintyre@strath.ac.uk

 ©2010 The American Physical Society

II. THE MODEL EQUATIONS

The model equations for a VCSEL with optical injection were introduced in [5]:

$$\begin{aligned}\partial_t E &= \varepsilon[E_I + P - (1+i\theta)E + i\nabla^2 E]\\ \partial_t P &= \xi(D)[(1-i\alpha)DE - P]\\ \partial_t D &= \sigma\varepsilon^2[J - D - \mathrm{Re}(EP^*) + d\varepsilon\nabla^2 D],\end{aligned} \tag{1}$$

where E and P are the cavity field and material polarization variables, respectively, D is the carrier density, ε is the cavity decay rate, E_I is the injected field, θ is the detuning between cavity and injection, α is the linewidth enhancement factor, $\sigma\varepsilon^2 = \gamma$ is the carrier decay rate, J is the injection current, d is the carrier diffusion constant, and Re(.) is the real part. Moreover (see [5]),

$$\xi(D) = \Gamma(D)[1 - i\alpha] + 2i\delta(D), \tag{2}$$

with $\Gamma(D) = 0.276 + 1.016D$ and $\delta(D) = -0.169 + 0.216D$. Diffraction is described by the Laplacian operator ∇^2 in two transverse dimensions (2D) and by $\partial_x^2 = (\partial^2/\partial x^2)$ in one transverse dimension (1D). Time has been scaled to the polarization decay time (typically of order 10^{-13} s), while the spatial scale is the square root of the diffraction parameter (typically of the order of 4 to 5 μm).

This model generalizes those adopted for the study of CS in absorbing or amplifying media below threshold [4] by including an equation for the dynamical evolution of the effective polarization variable P. This change is essential in order to avoid the unphysical short-wavelength instabilities that would appear below the injection locking point, where the homogeneous solution is unstable. Yet, the inclusion of the fast dynamics of P introduces a large separation of the time scales that makes the complete model (1) numerically stiff, resulting in inefficient simulation codes. For example, the typical orders of magnitude of the decay rates ε and $\gamma = \sigma\varepsilon^2$ are 10^{-2} and 10^{-4}, respectively.

We have shown previously that it is possible to drastically reduce simulation times of VCSELs and other solid-state lasers, without losing physical insight, by applying peturbative methods based on the center manifold theory [12]. These methods reduce the number of dynamical variables and consequently eliminate a significant amount of the numerical stiffness. The procedure is sketched in the Appendix, where the reduced equations for a VCSEL with optical injection, previously unreported, are obtained.

In this article, however, we consider the specific case of small pump current, J, and sufficiently high injected amplitude, E_I, to ensure that the VCSEL operates beyond the injection locking point, where the lower branch of the homogenous solution, which constitutes the background for the CS, is stable [5].

In this case the CS are stationary solutions of the complete model that can be described accurately even by reduced equations obtained at the lowest order in the perturbation parameter ε:

$$\begin{aligned}\partial_{\varepsilon^{3/2}t} E &= \frac{E_I - i(\alpha+\theta)E + i\partial_x^2 E}{\sqrt{\varepsilon}} + (1-i\alpha)WE\\ \partial_{\varepsilon^{3/2}t} W &= \sigma[J - (1+\sqrt{\varepsilon}W)(1+|E|^2)],\end{aligned} \tag{3}$$

where the population variable W has been defined via $D = 1 + \sqrt{\varepsilon}W$. It is interesting to note that at this perturbation order the semiconductor susceptibility is well described by the linewidth enhancement factor α and diffusion effects can be neglected.

The reduced model (3) is capable of accurately reproducing the results described in [5] in the case of stable homogeneous backgrounds, but with a reduction in CPU time by a factor between 100 and 300, similar to that observed in [12].

In the following we describe the effect of spatial variations of the phase of the injected field to realize and optimize an all-optical delay line based on a CS laser. We consider the effect of two types of phase modulations, sinusoidal and triangular (in both 1D and 2D), as shown:

$$E_I = |E_I| \exp[i\mu \sin(kx)] \tag{4a}$$

$$E_I = |E_I| \exp\left\{i\frac{2}{\pi}\mu \sin^{-1}[\sin(kx)]\right\} \tag{4b}$$

$$E_I = |E_I| \exp\left\{i\frac{2}{\pi}\mu \sin^{-1}[\sin(kx)\sin(ky)]\right\}. \tag{4c}$$

In each case, by varying the amplitude of the phase modulation, μ, it is possible to control the gradient applied to the CS and thus vary its transverse speed. By adjusting the wave vector, k, it is possible to control the total distance traveled by each CS. In principle, amplitude gradients and amplitude modulations are also possible but they are far less efficient and more unstable than phase modifications of the optical injections.

Note that under the action of phase gradients the CS are no longer stationary solutions of the equations and they can undergo relatively fast changes, especially when they merge. We have checked that the dynamics is still described accurately by Eqs. (3) by comparing them with the higher-order equations in ε of the Appendix.

III. WRITING LASER CAVITY SOLITONS

Writing CS in the VCSEL is the first operation of an all-optical delay line; the pulsed input signal is transferred to dissipative solitons that drift in the transverse direction of the laser. Figure 1 shows the intensity, phase, and carrier distributions of a steady-state CS in both 1D and 2D for parameter values where the lower homogeneous steady state is stable (see [5] for a steady-state stability curve). Note that the peak intensity of the 2D CS is higher than that of the 1D case because of the well-known larger self-focusing effect in two transverse dimensions. When writing CS, various parameters can affect the time required for a CS to fully establish. In particular, we consider the amplitude and the duration of the address beam. We have performed numerical simulations of Eqs. (3) to evaluate the *minimum* duration of the address beam required to establish a CS in the VCSEL with optical injection as a function of the amplitude of the address beam. In Fig. 2 we compare the results for the cases below threshold (amplifier $J = 0.96$) and above threshold ($J = 1.05$) and find that there is a clear advantage in the response of the delay line when operating the VCSEL above threshold.

The minimum injection time for writing a CS is, however, not necessarily the optimum one because of the switch-on dynamics of the generated CS. In Fig. 3 we show that for a fixed value of the amplitude of the writing beam (0.65) an

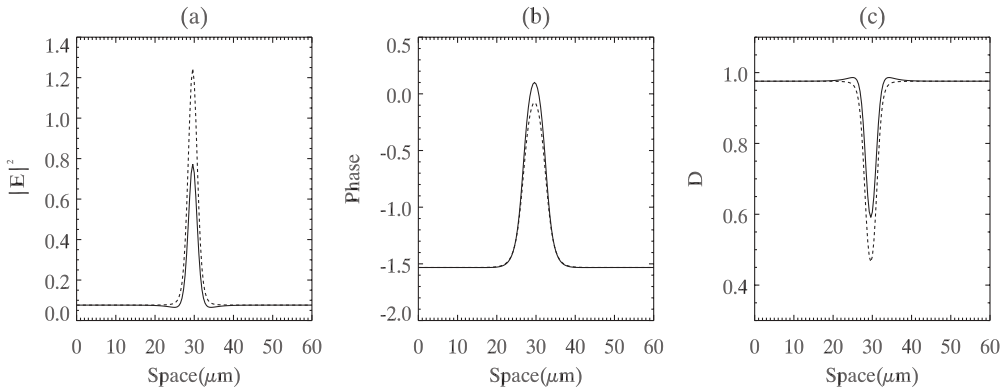

FIG. 1. Spatial distributions of (a) the intensity, (b) phase, and (c) carrier density of a laser CS in a VCSEL with injection. Solid (dashed) lines are for the 1D (2D) case. Parameters are $J = 1.05$, $\varepsilon = 0.04$, $\gamma = 10^{-4}$, $|E_I|^2 = 0.03$, $\theta = -2.3$, and $\alpha = 3.0$.

increase in the address beam duration from 0.15 to 0.20 ns leads to a considerably faster establishment of the CS, from around 5 ns to around 1 ns. However, further increases of the duration of the writing beam do not further reduce the CS establishing time. Figure 3 shows, for example, that for an address pulse duration of 0.5 ns (dot-dash line) the establishment of the CS takes around 1.8 ns. This is typical of the critical behavior of CS switching as originally described and observed in a liquid-crystal light valve [2,13].

Although the writing speed of CS is an important feature in the optimization of the operation of an all-optical delay line, the minimum repetition rate of the input signal is limited by how quickly CS can be moved away from the writing position while remaining independent from each other. CS are moved away by a phase gradient that both induces their motion and provides the delay. Note that in this section we discuss the use of phase gradients to achieve the maximum repetition rate while in Sec. IV we present the use of such gradients to introduce delay.

The use of a sinusoidal phase modulation of the injected field [see Eq. (4a)] to quickly remove CS from the writing position is not optimal since the gradient is constantly decreasing toward the modulation peak, causing the CS velocity to decrease and CS to merge with each other. Simulations with a sinusoidal phase modulation of amplitude $\mu = 1$ show that up to 200 ns are required between CS writing cycles. Replacing the sinusoidal phase modulation (4a) with a triangular phase modulation (4b), however, eliminates this problem as it provides a constant gradient and a constant velocity as the CS proceed toward the modulation peak. This fact, coupled with the absence of spatial oscillations in the CS tails in our CSL, allows for much faster repetition rates of up to 1 ns between successive pulses. Figure 4 shows the maximum data transmission rate with an all optical delay line based on a CSL for a range of values of the modulation amplitude, μ, and a fast carrier decay rate of $\gamma = 10^{-3}$.

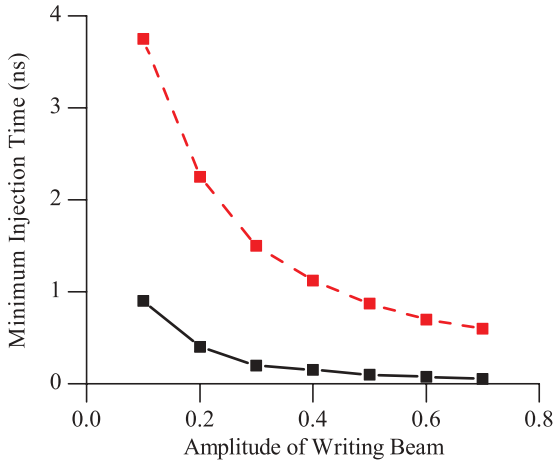

FIG. 2. (Color online) Qualitative comparison between the minimum injection time required to write a CS in the VCSEL [black (solid) line, $J = 1.05$] and amplifier [red (dashed) line, $J = 0.96$] cases for varying amplitudes of the address beam, 1D case. Similar results have been obtained for the 2D case. Other parameters for the lasing case are fixed to the values given in Fig. 1. The parameters for the amplifier are $E_I = 0.61$, $\theta = -2.25$, and $\alpha = 4.5$.

IV. MOTION OF LASER CAVITY SOLITONS

Once CS have been written in a VCSEL with optical injection, their motion is affected by the dynamics of the background. In fact, depending on the parameters (in particular, the pumping current), CS can either have a stable

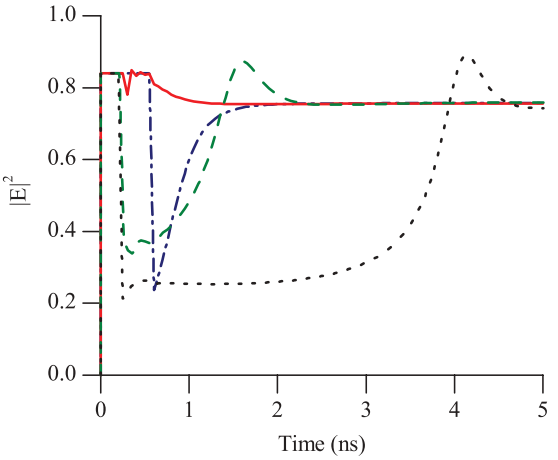

FIG. 3. (Color online) CS peak intensity during and after writing via an address beam of amplitude 0.65 and various durations. Dotted line (black), duration = 0.15 ns; dash line (green), duration = 0.16 ns; solid line (red), duration = 0.20 ns; dot-dash line (blue), duration = 0.50 ns. Parameters are those of Fig. 1.

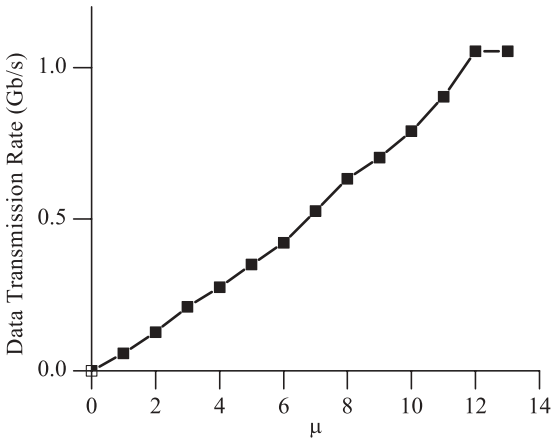

FIG. 4. Data transmission rate with varying amplitudes of the triangular phase-modulation of the injected field. Here, $\gamma = 10^{-3}$ and other parameters are those of Fig. 1.

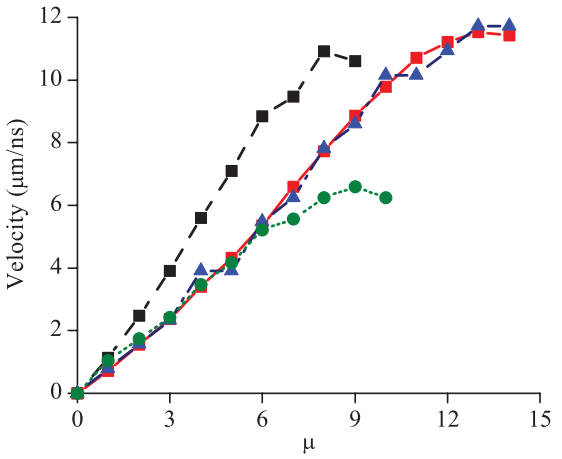

FIG. 5. (Color online) CS velocity as a function of the amplitude of the phase modulation of the injected field. The motion induced by a sinusoidal modulation is shown by the dashed (black with squares) line while the motion induced by a triangular modulation is shown by the solid (red with squares) line in 1D and by the dotted (green with circles) line in 2D. Further, the dot-dashed (blue with triangles) line shows the velocity calculated using the full model (1) and a triangular phase modulation. Here $\gamma = 10^{-3}$, $k = 0.036$, and other parameters are those of Fig. 1.

background (similar to the case below threshold) or sit on a rapidly oscillating unstable background [5]. Here we have induced CS motion by a modulation of the phase of the injected signal in the regime where the background is stable.

Spatially periodic modulations of the phase of the injected field provide a versatile and effective method for multiple delay lines within the same device. Periodic modulations of the injected phase extend over a wide range of parameters where both the system and CS remain more stable than the cases, for example, of modulating injected amplitudes or detunings. Parallel delay lines can be implemented by using several modulations of the phase across the transverse length of the VCSEL.

By varying the amplitude of the phase modulation, μ, it is possible to control the gradient applied to the CS and hence its velocity, as shown in Fig. 5 in both 1D and 2D configurations. Adjustments of the wave vector, k, control the total distance traveled by the CS. Note that, although a sinusoidal modulation can produce a larger peak velocity than a triangular modulation, a triangular modulation is preferable since it provides a constant gradient and therefore a constant velocity until a CS reaches the peak. This can help in reducing unwanted interactions of the CS before they reach the modulation peak where the readout operation is performed. The motion of dissipative solitons with triangular modulations has been realized and investigated in liquid-crystal light valves [14].

Varying the carrier decay rate, γ, provides another method for controlling the velocity of the CS [11], while keeping both μ and k constant. The increase in velocity is basically inversely proportional to the decay time of the carriers (see Fig. 6 for 1D simulations). If γ is too small, however, the system does not support CS, while if it is too large CS will begin to form randomly across the cavity width. Note that the range and stability of the CS upon variations of γ is reduced by an order of magnitude in our active VCSEL in comparison with that seen below lasing threshold, where CS have a more stable background [11]. Similar results have also been obtained in 2D.

V. READOUT OPERATION: MERGING OF LASER CAVITY SOLITONS

One of the most difficult operations in an optical memory based on CS is that of collecting the information stored in a CS. This is generally achieved by using readout pulses with suitable phase and position that are capable of erasing the CS. In delay lines, the readout operation can be perfomed by using localized detectors that collect the output intensity of a traveling CS. We propose, in this section, an alternative readout operation that does not require small detectors and that is based on the self-erasing mechanism of CS merging at the peaks of the modulations. Induced collision of diffractive autosolitons has been described in pioneering numerical simulations of systems with two homogeneous states for the implementation of optical adders (not to be confused with optical snaking) [15]. In this case the collision between a larger and a smaller autosoliton destabilizes the domain walls that connect the two homogeneous states leading to the survival of just one of the

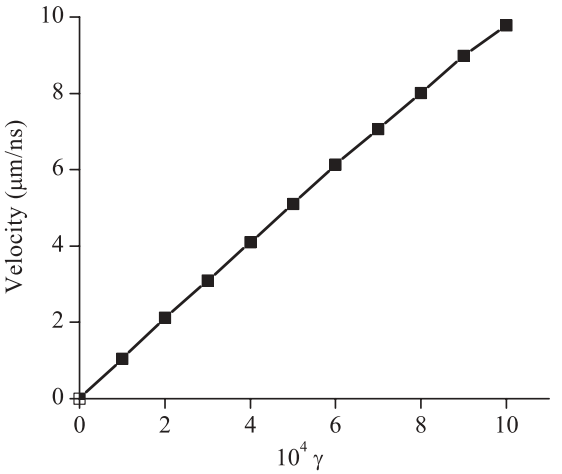

FIG. 6. CS velocity as a function of the decay rate of the carriers, γ, for a VCSEL with optical injection. Here $\mu = 10$, $k = 0.036$, and other parameters are those of Fig. 1.

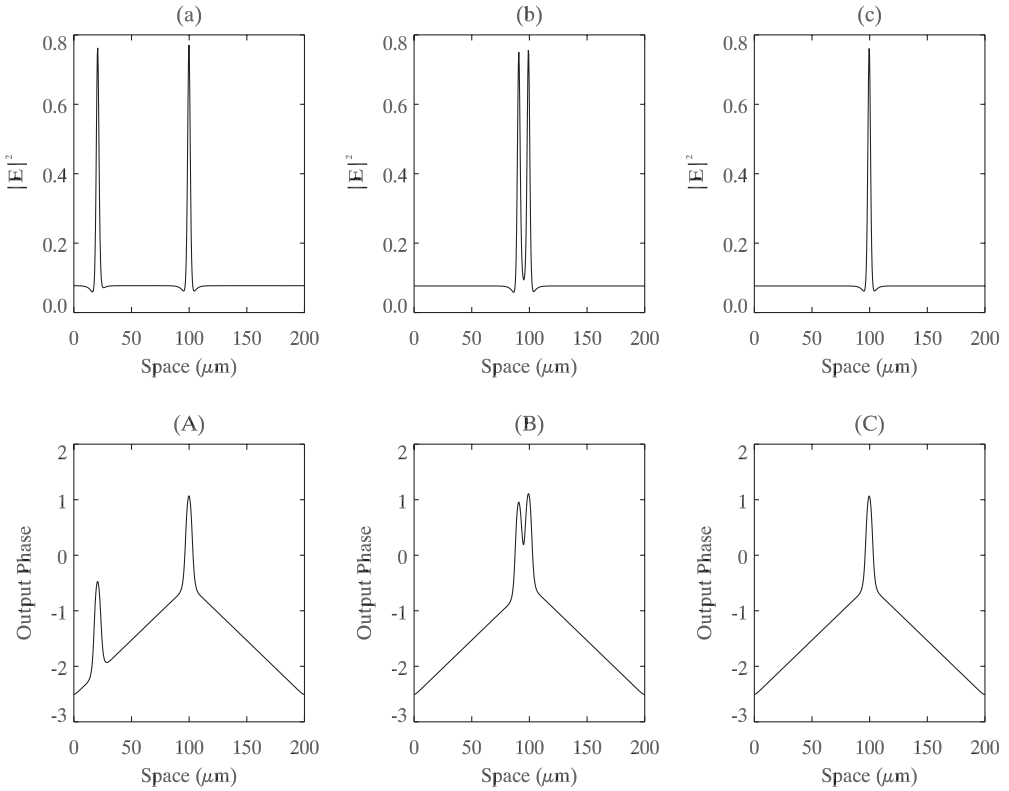

FIG. 7. Merging of two CS in a VCSEL with triangular phase modulation of the optical injection. Panels (a)–(c) display the spatial profile of the laser intensity, while panels (A)–(C) show the phase of the output field. Here $\mu = 1.0$, $k = 0.036$, and the other parameters are those of Fig. 1. (a) and (A) correspond to $t = 0$ ns, (b) and (B) correspond to $t = 870$ ns, and (c) and (C) correspond to $t = 990$ ns.

colliding solitons [15]. Collisions leading to destabilization of domain walls can also be induced by noise [16]. In the case of CS in VCSELs with optical injection, there is no bistability between homogeneous states and no domain walls connecting them. The merging mechanism of CS described here is related to the absorption of energy from the pump and its release in the form of short pulses. To investigate the self-erasing mechanism of CS merging, extensive simulations have been performed to describe the interactions of CS around a single maximum of the phase modulation. For example, Fig. 7 shows the effect of a second CS on an initial CS already positioned at a maximum of the phase modulation. Here we have used a triangular phase modulation of the injected field to induce CS motion. A clear merging process takes place at the peak of the modulation.

Simulations over a wide range of the amplitude of the phase modulation, μ, display CS merging at the peak of the phase modulation, as shown in Fig. 7. This occurs even for very small values of μ, corresponding to small spatial gradients, very low velocities of the CS, and large delays in the delay line.

When more than two CS are introduced in the VCSEL, they all move toward their nearest respective peak of the injected phase modulation and, when two or more meet, they merge to form a single CS (see Fig. 8).

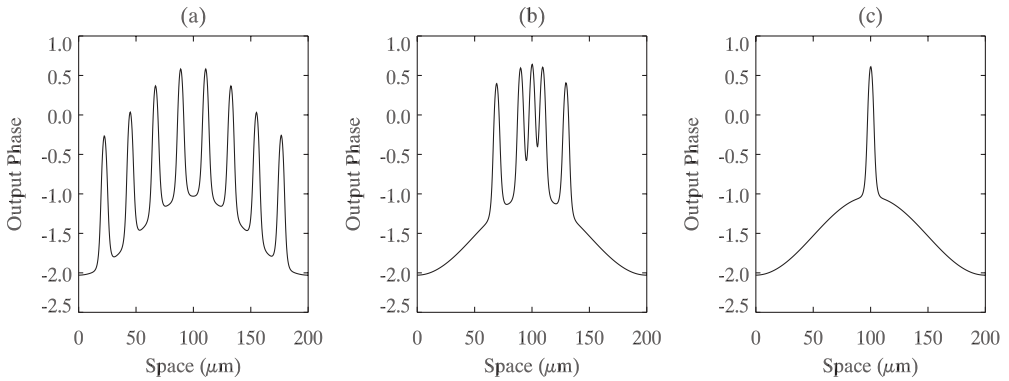

FIG. 8. Merging of eight CS in a VCSEL with sinusoidal phase modulation of the optical injection. The phase of the output field is plotted versus the transverse spatial coordinate. Here the phase modulation of the injected field corresponds to $\mu = 0.5$ and $k = 0.036$ and is switched on after a comb of eight equally spaced CS has been initiated. The other parameters are those of Fig. 1. (a) corresponds to $t = 0$ ns, (b) corresponds to $t \approx 838$ ns, and (c) corresponds to $t \approx 2488$ ns.

CS merging is commonplace in CSL over a wide range of the modulation parameters. It can be used in the readout operation of a delay line since one CS is removed from the VCSEL at each merging process in a way similar to the use of external erasing beams.

CS soliton merging also eliminates soliton clogging, which can be detrimental at the output of optical delay lines based on amplifiers. This feature can thus be beneficial to the practical implementation of all-optical delay lines in CSLs.

The process of merging of dissipative spatial solitons is quite intriguing and deserves special attention. Here, for example, we demonstrate that during merging there is the emission of light pulses accompanied by the violation of an energy balance.

We consider first the simpler case of laser CS without dynamical contributions of the carrier population. By setting the population variable D to its equilibrium value, one obtains

$$\begin{aligned} \partial_{\varepsilon t} E &= E_I - i(\theta+\alpha)E + i\partial_x^2 E + (1-i\alpha)(D-1)E \\ D &= \frac{J}{1+|E|^2}. \end{aligned} \tag{5}$$

In analogy with the cubic-quintic Ginzburg-Landau equation [17], we introduce a continuity equation for the field E:

$$\frac{\partial \rho}{\partial t} + \frac{\partial j}{\partial x} = Q, \tag{6}$$

where the density is $\rho = |E|^2$ and the current is $j = i(E\partial_x E^* - E^*\partial_x E)$. For conservative systems, the quantity Q is identically zero. For injected and dissipative systems like (5), however, we can write

$$Q = 2[\mathrm{Re}(E_I E^*) + D|E|^2 - |E|^2]. \tag{7}$$

The three contributions that form Q are identified as the energy provided by the external injection, the energy stored in the material by the laser pumping, J, and the losses at the laser output, respectively. Q is trivially equal to zero for homogeneous steady states while the spatial part $\partial_x j$ counterbalances Q locally for stationary CS. In this last case, however, the integration over the full transverse space of Q (as well as $\partial_x j$) is identically zero and one talks of "energy balance" across the full profile of a CS.

We find that the energy balance for $\int Q dx$ persists in the case of CS moving on phase gradients. At the moment of the merging, however, clear violations appear. Figure 9 shows the time evolution of the energy balance before and after a CS merging event for the single equation model (5). Balance takes place both during the motion of one CS toward the second and after the collision event. Around the merging time, however, energy exchanges are clearly not balanced. Initially, excess energy is absorbed from the injection to be later released through cavity losses. Note that this excess energy is not stored in the carrier distribution but is instead emitted from the VCSEL in the form of a short pulse, as shown in the inset of Fig. 9.

The physical description of CS merging in model (3) is more complicated due to the delayed dynamics of the carriers. When we take this into account, the density term in the continuity equation (6) becomes $\rho = |E|^2 - D^2$ while the current term, $j = i(E\partial_x E^* - E^*\partial_x E)$, is unchanged. There

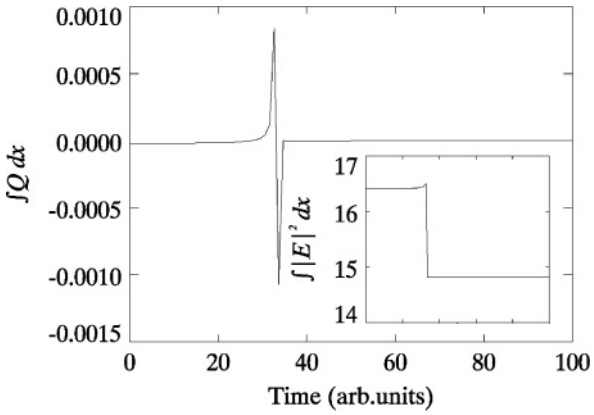

FIG. 9. Time evolution of the energy balance $\int Q dx$ for the merging of two CS in the model (5). (Inset) Cavity losses $\int |E|^2 dx$ as a function of time (with scale as in the main image). Parameters are those of Fig. 1. Triangular modulation parameters are $\mu = 0.1$ and $k = 0.036$.

is a simple explanation for the negative sign in front of the carrier term, D^2, in the definition of ρ: In contrast with the peak of the field intensity, the carrier distribution has a trough

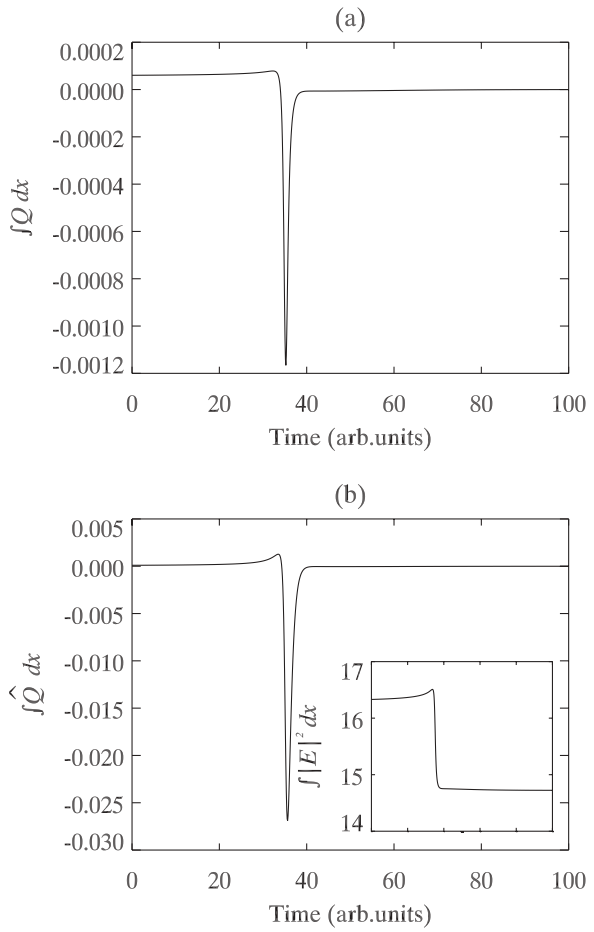

FIG. 10. Time evolution of (a) the quantity $\int Q dx$ without the carrier density dynamics and (b) $\int \hat{Q} dx$ with the carrier density dynamics for the merging of two CS in the model (3). (Inset) Cavity losses $\int |E|^2 dx$ as a function of time (with the scale as in the main image). Parameters are those of Fig. 1. Triangular modulation parameters are $\mu = 1.0$ and $k = 0.036$.

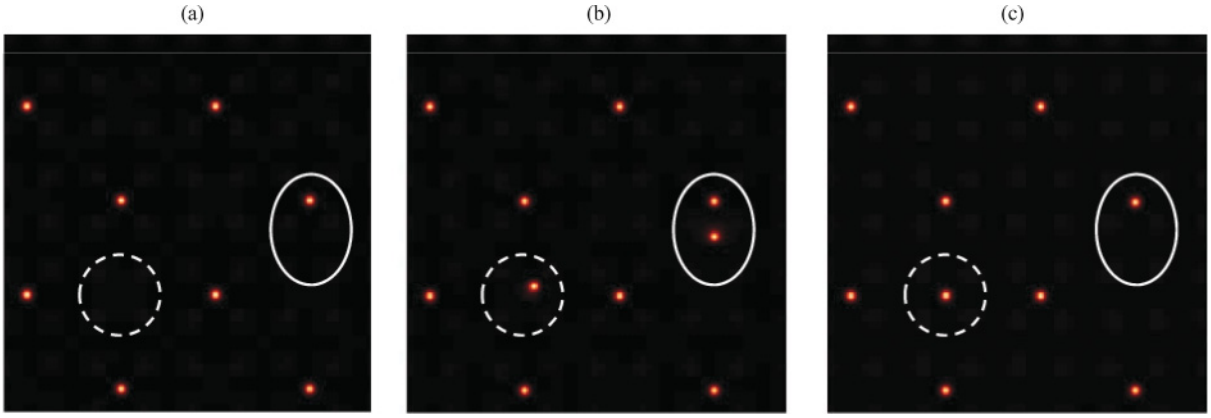

FIG. 11. (Color online) Motion and merging of CS in a VCSEL with phase modulation of the optical injection in 2D given by (4c). (a) The stationary 2D distribution of the output intensity before the writing of two new CS. (b) The distribution immediately after the writing of the two CS and (c) after $t = 27.5$ ns from the writing of the two new CS. The CS in the dashed circle moves to the closest maximum of the modulation while the CS in the solid oval merges with a CS at the peak of the phase modulation.

at the center of the CS [see Fig. 1(c)]. This means, for example, that field dissipations are larger at the center of the CS while the carrier dissipations are reduced in the same place due to inhibited spontaneous emission. For Eqs. (3), the definition of Q then has to be updated to [18]

$$\frac{\partial(|E|^2 - D^2)}{\partial t} + \frac{\partial j}{\partial x} = \hat{Q} \tag{8}$$
$$= 2\{\mathrm{Re}(E_I E^*) + (D-1)|E|^2 + \sigma[D(1+|E|^2) - J]\}.$$

The addition of the carrier dynamics corresponds to the term multiplied by σ in the definition of $\hat{Q}$. Again, $\hat{Q}$ is identically equal to zero for homogeneous steady states while $\int \hat{Q}dx = 0$ for a stationary CS due to energy balance. Figure 10(a) shows the time evolution of the quantity $\int Q dx$ with Q from Eq. (7), that is, without the carrier dynamics term, before and after a CS merging event for the model (3). The inclusion of the carrier dynamics in the definition of $\hat{Q}$ ensures balance during the motion of one CS toward the second [see the comparison between Figs. 10(a) and 10(b)]. As in the previous case, energy exchanges are clearly not balanced around the merging of CS since excess energy is first absorbed from the injection and later released through cavity losses. Again, the excess energy is emitted from the VCSEL in the form of light pulses, as shown in the inset of Fig. 10(b).

CS merging is also observed in simulations with two transverse dimensions. Figure 11 shows an example where two newly written CS move toward their closest maximum of the triangular phase modulation (4c) in a 2D lattice. When the maximum is empty, the CS is properly positioned. Where the maximum is occupied by another CS, merging takes place. Such mechanisms can be of practical use in the experimental implementation of 2D optical memories.

Finally, we note that 1D and 2D CS in VCSELs with optical injection have tails with almost no spatial oscillations. This fact greatly reduces the interaction between CS, resulting in the merging of CS described above and in maintaining a constant temporal separation between input pulses during their motion. Both effects are beneficial for the implementation of a delay line and for applications in optical information processing.

VI. CONCLUSIONS

We have demonstrated that the concept of an all-optical delay line based on CS can be extended from absorbing or amplifying media kept below the laser threshold to lasing media. We have shown that the position, velocity, and merging of CS in a VCSEL with optical injection are easily controlled optically by introducing linear gradients or periodic modulations of the phase of the injected field. The CS velocity, and consequently the delay in all-optical delay lines, can be controlled by varying the gradient, the amplitude, and the spatial wave vector of the phase modulation, as well as the response time of the medium. The VCSEL operator can control spatially modulated optical injections in order to select CS traveling distances and hence form CS arrays for optical memories. When two or more CS meet at a peak, they merge to form a single CS. The merging processes release short pulses of light that can be used in the readout operation of the delay line. They also help eliminate the detrimental phenomenon of CS clogging.

The minimum time required for a CS to completely establish in a VCSEL is predicted to be less than a nanosecond. Consequently, the only factor limiting the speed of performance of the delay line is how quickly CS can be maneuvered from the path of the writing beam. By introducing a triangular, rather than a sinusoidal, phase modulation, the velocity of the CS remains constant until it reaches the peak. The minimum time required before introducing a further CS varies depending on the delay required and ranges from approximately one to tens of nanoseconds depending on the response time of the semiconductor material.

We expect delay lines based on CS motion to work in other active configurations such as those based on frequency-selective feedback [8,19] and mutually coupled semiconductor microresonators [9]. Extensions to systems based on media different from semiconductors, such as liquid-crystal light valves [14,20] and photorefractives, are also feasible.

ACKNOWLEDGMENTS

We thank the European Commission for financial support through the FunFACS and HIDEAS collaborations. We thank W. J. Firth and T. Ackemann for useful discussions.

APPENDIX

Following the approach of [12], it is possible to take advantage of the separation of the time scales between the different variables to obtain reduced equations that capture the long-term spatiotemporal dynamics of the system. We do not enter into the details of the procedure to avoid repetition but write the final equations that apply to the case with injection and that were not reported before [12]. By considering ε, the ratio between the cavity and polarization decay rates, as the perturbation parameter, reduced equations at first order in ε are given by

$$\partial_{\varepsilon^{3/2}t} E = \frac{E_I - i(\alpha+\theta)E + i\partial_x^2 E}{\sqrt{\varepsilon}} + (1 - i\alpha)WE + \sqrt{\varepsilon}(1 - i\alpha)(1 + \sqrt{\varepsilon}W)(\mathcal{L}E + Z) \tag{A1}$$

$$\partial_{\varepsilon^{3/2}t} W = \sigma\{J - (1 + \sqrt{\varepsilon}W)(1 + |E|^2) - \varepsilon \mathrm{Re}[(1 - i\alpha)E^*(\mathcal{L}E + Z)] + d\varepsilon^{3/2}\partial_x^2 W\}$$

$$\mathcal{L} = -\frac{i\partial_x^2}{\xi(1) + i\varepsilon\partial_x^2}$$

$$Z = -\frac{1}{\xi(1)}[E_I - i(\alpha+\theta)E + \sqrt{\varepsilon}(1 - i\alpha)WE],$$

where $D = 1 + \sqrt{\varepsilon}W$. Note that the operator $\mathcal{L}$ has not been expanded further in ε for numerical convenience. Equations (3) can be easily obtained from Eqs. (A1) keeping only terms up to order ε^0 in the equation for E and order $\varepsilon^{1/2}$ in the equation for W. This corresponds to a standard adiabatic elimination of the variable P. Equations (3) reproduce accurately all the stationary solutions of the complete model. Yet, Eqs. (A1) contain, through the term $\mathcal{L}E + Z$, corrections to the standard adiabatic elimination that suppress any unphysical behavior arising in the dynamics of the CS due to the oversimplified form of the susceptibility in Eqs. (3). We have used them to check that the description given by Eqs. (3) remains accurate even in presence of the dynamics induced by the phase gradients.

[1] T. Ackemann and W. J. Firth, in *Dissipative Solitons*, edited by N. Akhmediev and A. Ankiewicz (Springer, Berlin, 2005).

[2] T. Ackemann, W. J. Firth, and G.-L. Oppo, Adv. At. Mol. Opt. Phys. **57**, 323 (2009).

[3] B. Schapers, M. Feldmann, T. Ackemann, and W. Lange, Phys. Rev. Lett. **85**, 748 (2000).

[4] S. Barland, J. R. Tredicce, M. Brambilla, L. A. Lugiato, S. Balle, M. Giudici, T. Maggipinto, L. Spinelli, G. Tissoni, T. Knödl, M. Miller, and R. Jäger, Nature (London) **419**, 699 (2002).

[5] X. Hachair, F. Pedaci, E. Caboche, S. Barland, M. Giudici, J. R. Tredicce, F. Prati, G. Tissoni, R. Kheradmand, L. A. Lugiato, I. Protsenko, and M. Brambilla, IEEE J. Sel. Top. Quantum Electron. **12**, 339 (2006).

[6] X. Hachair, G. Tissoni, H. Thienpont, and K. Panajotov, Phys. Rev. A **79**, 011801(R) (2009).

[7] Y. Tanguy, T. Ackemann, and R. Jäger, Phys. Rev. A **74**, 053824 (2006).

[8] Y. Tanguy, T. Ackemann, W. J. Firth, and R. Jäger, Phys. Rev. Lett. **100**, 013907 (2008).

[9] P. Genevet, S. Barland, M. Giudici, and J. R. Tredicce, Phys. Rev. Lett. **101**, 123905 (2008).

[10] W. J. Firth and A. J. Scroggie, Phys. Rev. Lett. **76**, 1623 (1996).

[11] F. Pedaci, S. Barland, E. Caboche, P. Genevet, M. Giudici, J. R. Tredicce, T. Ackemann, A. J. Scroggie, W. J. Firth, G.-L. Oppo, G. Tissoni, and R. Jäger, Appl. Phys. Lett. **92**, 011101 (2008).

[12] G.-L. Oppo, A. M. Yao, F. Prati, and G. J. de Valcarcel, Phys. Rev. A **79**, 033824 (2009).

[13] A. Schreiber, M. Kreuzer, B. Thüring, and T. Tschudi, Opt. Commun. **136**, 415 (1997).

[14] B. Gütlich, H. Zimmermann, C. Cleff, and C. Denz, Chaos **17**, 037113 (2007).

[15] N. N. Rosanov, Opt. Spectrosc. **72**, 243 (1992); N. N. Rosanov, A. V. Fedorov, S. V. Fedorov, and G. V. Khodova, Proc. SPIE **2039**, 330 (1993).

[16] I. Rabbiosi, A. J. Scroggie, and G.-L. Oppo, Phys. Rev. Lett. **89**, 254102 (2002); Phys. Rev. E **68**, 036602 (2003).

[17] N. Akhmediev and A. Ankiewicz, in *Dissipative Solitons*, edited by N. Akhmediev and A. Ankiewicz (Springer, Berlin, 2005).

[18] Note that terms in ε in Eqs. (A1) provide negligible contributions to the continuity equation and integrate to zero over the spatial variable.

[19] A. J. Scroggie, W. J. Firth, and G.-L. Oppo, Phys. Rev. A **80**, 013829 (2009).

[20] C. Cleff, B. Gütlich, and C. Denz, Phys. Rev. Lett. **100**, 233902 (2008).